The Influence of the Corrosion and Temperature on the Von Mises Stress in the Lateral Cover of a Pressurized Fuel Tank

Assoc. Prof. PhD. Eng. **Mihai ŢĂLU**

University of Craiova, Faculty of Mechanics, Department of Applied Mechanics and Civil Engineering, Calea București Street, no. 107, 200512 Craiova, Dolj county, Romania. E-mail: mihai_talu@yahoo.com

Abstract: *The objective of this study was to evaluate the effect of the corrosion and temperature on the state of stress in the lateral cover of a pressurized fuel tank of AISI 4340 steel used in automotive industry. This analysis of the Von Mises stress laws variation in the lateral cylindrical cover with the corresponding CAD solutions and results of simulations will improve the design and performances of the pressurized fuel tank during the exploitation period. Furthermore, it offers design guidance for pressurized fuel tank durability in the early stages of product development to reduce overall new product development costs significantly.*

Keywords: *Automotive industry, corrosion, cylindrical cover, industrial engineering design, optimization methods, pressurized fuel tank, state of effort*

1. Introduction

One of the most dynamic sectors of the economy is that of automotive construction [1-4].
A pressurized fuel tank has the role of safely storing and supplying fuel to the engine [5-9].
Optimum tank design with reduced production costs and start-up time in manufacturing is key to competition in the automotive market [10-13]. Pressurized fuel tanks have complex geometries and are especially made of steel or aluminum [5, 6, 8-13].
For tanks of storing compressed natural gas (CNG) fuel, the maximum pressure test is at p = 300 bar, while pressures for liquefied petroleum gas (LPG) storage are 10 times lower [5, 6, 9].
Currently, various design methods [14-20] and data analysis techniques for both quantitative and qualitative research [21-34] as well as recommendations from renowned researchers are used in the computer engineering design and manufacturing process of pressurized fuel tanks [35-37].
The use of these pressurized fuel tanks in the automotive mass production was made after some new modifications in the design of the machines, which led to increased safety and reliability in operation [5, 6], using a computer-based information system [38].
The CAD study allows for the establishment of high stress states, after which the presurized fuel tanks are redesigned to admisible values to meet the optimization criteria imposed [39-41].

2. The optimal design of lateral cover of the cylindrical pressurized fuel tank

The main structural elements which make up a pressurized cylindrical tank are shown in Figure 1.
In this study it is considered that the corrosion action is uniform and takes place only on the interior surfaces of the pressurized fuel tank where the CNG or LPG fuel is in contact with them, being considered as an aggressive chemical environment.

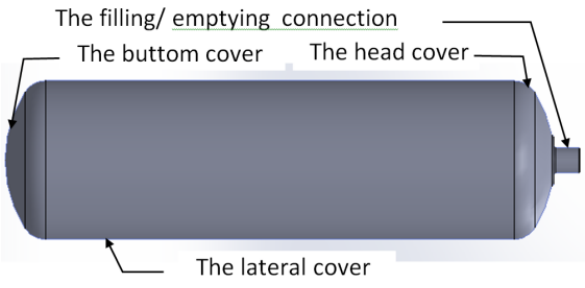

Fig. 1. Pressurized cylindrical fuel tank

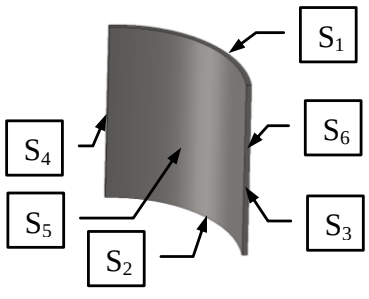

Fig. 2. The outer surface of the pressurized fuel tank

On the outer surface of the tank (Figure 2), the corrosion is attenuated by the paint protective layers which are applied against the aggression of the agents from the external environment.
The CAD optimal design of the lateral cover of the pressurized fuel tank permits to determine the thickness of the lateral cover to resist to the required demands, starting from the following initial data:
- the lateral cover has: the external diameter of D = 250 mm and the length of L = 700 mm;
- the maximum hydraulic pressure test is: p_{max} = 30 N/mm^2;
- the ambient environment temperature varies between the limits: T = -30 ^{0}C,..,+60 ^{0}C;
- the material of tank is made from AISI 4340 steel.

From the analysis of the constructive form it was found that the cover has an axial symmetry (according to Figure 1), which allows us to use in the calculations of a parameterized model with section at ¼ of the initial model (according to Figure 2).
Initially parameterized modeling of the pressurized cylindrical tank was done in the AutoCAD Autodesk 2017 software [42], which was imported to SolidWorks 2017 software [43] for analysis with the: Static, Thermal and Design Study modules.
The parameterized model was applied to the surfaces specified in Figure 2 (load forces, link restrictions) and symmetry conditions (as shown in Figures 3 to 6):
- maximum loading pressure on the inner surface, S_5: p_{max} = 30 N/mm^2, (according to Figure 3);
- thermal loading on the outer surface S_6, with variation between the limits: T = -30^0,.., +60^0, (as shown in Figure 4);
- opposing and equal traction forces on the surfaces: S_1 and S_2 given by the pressure action on the inner surfaces of the end covers with the value of: F = p_{max} (π R^2)/4 = 367969 N, (Figure 5);
- symmetry conditions on the surfaces: S_1 and S_2;
- the null displacement of the cover in the direction of the symmetry axis.

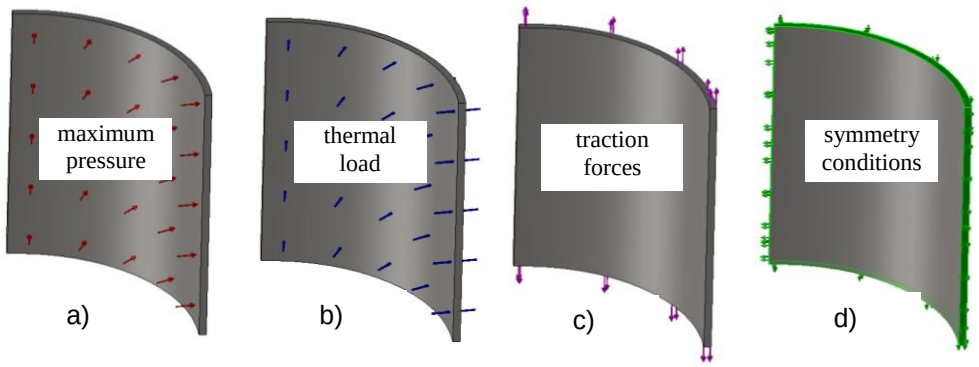

Fig. 3. a) The loading pressure on the inner surface S_5; b) The thermal load on the outer surface S_6; c) The traction forces on the surfaces S_1 and S_2; d) The symmetry conditions on surface S_1 and S_2

In the calculation the parameter under optimization is defined as the thickness of the cover with continuous variation between the limits: s = 4…7 mm. Namely, the temperature is considered to be continuously variable between the limits of the exploitation range: T = -30 ^{0}C, .., +60 ^{0}C.
The goal optimization function is defined as a target to achieving a minimum mass.
As a calculation restriction it was imposed that the Von Mises resulting stress must be less than or equal to the permissible traction value of the material cover AISI 4340 steel, equal to σ_a = 710 N/mm^2.

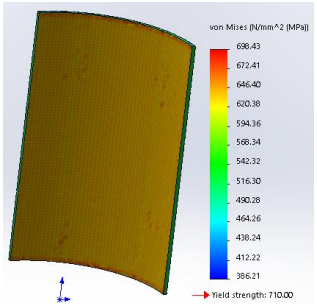

Fig. 4. The Von Mises stress at T = -30 ^{0}C

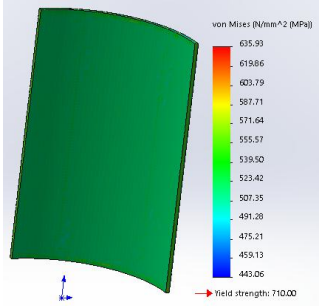

Fig. 5. The Von Mises stress at T = 60 ^{0}C

After the optimization calculation, the program gives a minimum thickness of s = 6.05 mm, for which we have a uniform Von Mises stress of σ_{max}= 698.43 N/mm^2 value at the temperature of T = -30 ^{0}C, (as shown in Figure 4).
In the addition, for this thickness has been calculated the Von Mises stress at T = 60 ^{0}C, which has the σ_{rez} = 635.93 N/mm^2 value, and his distribution is shown in Figure 5.
Now, in order to resist to the entire exploitation interval by n_a = 20 years imposed from the design theme, the optimal thickness is corrected considering the influence of the corrosion and the negative tolerance of the metal sheet, using the following formula [5, 6]:

$$s_{real} = s_{opt} + \Delta s_c + \Delta s_T = s_{opt} + v_c \cdot n_a + abs(A_i) \quad (1)$$

where:

- Δs_c, the addition of thickness due to the corrosion of the laminate sheet;
- Δs_T, the addition of thickness due to the negative tolerance of the execution of laminate metal sheet;
- v_c, the corrosion rate of the cover with values between the limits: v_c = 0.1, ..., 0.15 mm/year, where we adopt the v_c = 0.12 mm/year;
- n_a, the number of years of exploitation; n_a = 20 years;
- A_i, the lower negative deviation of the laminate metal sheet; A_i = - 0.8 mm, for thicknesses between the limits: s = 8...12 mm.

By substituting the minimum thickness of the laminate sheet it is obtained has the following value:

$$s_{real\ min} = 6.05 + 0.12 \cdot 20 + abs(-0.8) = 9.25 \text{ mm} \quad (2)$$

For the execution, we choose a laminate sheet of AISI 4340 steel that has a thickness of $s = 10^{+0.3}_{-0.8}$ mm.

2.1. The CAD analysis of Von Mises stress in lateral cover

Knowing the complete geometry of the cover, the Von Mises stress calculation was further performed and it was found to have a maximum value at the temperature of T = -30 ^{0}C.
At the initial moment of exploitation, when n_a = 0 years, the thickness to be taken into account in the calculation has the value of s = 9.2 mm, where from the covering has subtract the negative deviation from the maximum thickness of the laminate sheet.
The maximum working pressure at which the cover can resist before the resultant Von Mises stress becomes equal with the admissible traction value of material, σ_a = 710 N/mm^2, has the value of p = 45.5 N/mm^2, showing the graph distribution from the Figure 6a.
The explosion pressure at this moment that occurs when touched the breaking stress of material σ_r = 1100 N/mm^2, has the value of p_r = 74.8 N/mm^2, (according to Figure 6b).

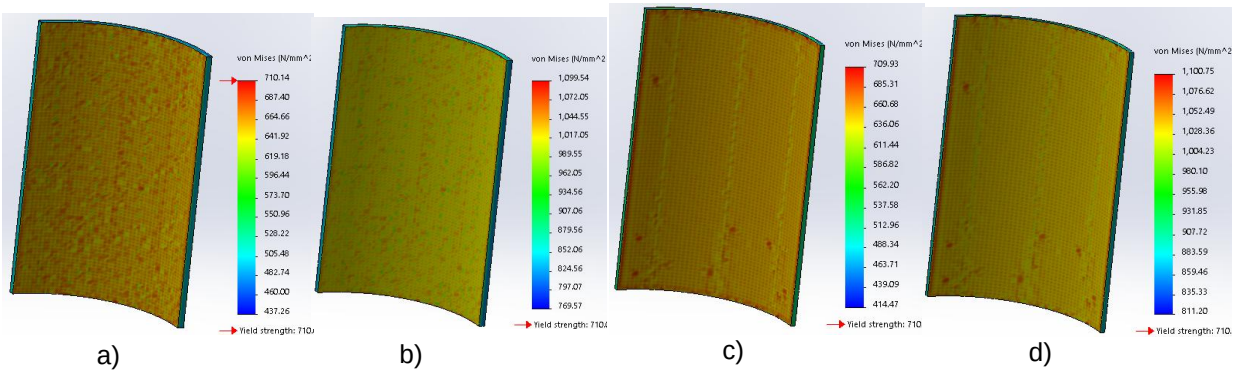

Fig. 6. a) The stress at maximum pressure, n_a = 0 year; b) The stress at explosion pressure, n_a = 0 year; c) The stress at maximum pressure, n_a = 20 years; d) The stress at explosion pressure, n_a = 20 years

By calculating the pressure value at the beginning and the end of the exploitation period when n_a = 20 years, after what the corrosion has reduced the thickness of the cover to s = 6.8 mm, the maximum working pressure is obtained for p = 34.5 N/mm^2, which has the stress distribution from

Figure 6c and for the value of the explosion pressure p_r = 57.75 N/mm^2, has the stress distribution shown in Figure 6d.
From the analysis of the results of corrosion influence at the end of the exploitation period when the thickness of the cover decreases by Δs = 26.09 %, the maximum working pressure decreased by Δp_{max}= 24.17 % and the explosion pressure decreased by Δp_r = 23.1 %.
The calculation made for determining the combined influence of the corrosion with temperature on the resulting stress Von Mises state, when loading the cover with the maximum hydraulic test pressure p_{max} = 30 N/mm^2, is given in Table 1.

Table 1: The influence of the corrosion with temperature on the resulting stress Von Mises state

		T [^{0}C]									
no. year	**s [mm]**	-30 ^{0}C	-20 ^{0}C	-10 ^{0}C	0 ^{0}C	10 ^{0}C	20 ^{0}C	30 ^{0}C	40 ^{0}C	50 ^{0}C	60 ^{0}C
		σ [N/mm^2]									
0	9.2	531.36	504.46	478.19	453.75	431.69	410.54	395.55	398.56	406.94	417.27
1	9.08	533.07	506.18	480.48	456.45	434.48	414.31	400.03	404.09	413.49	424.81
2	8.96	535.17	508.31	483.13	459.47	437.6	418.34	404.76	409.77	420.13	432.35
3	8.84	537.67	510.85	486.15	462.83	441.05	422.65	409.74	415.6	426.85	439.91
4	8.72	540.57	513.81	489.54	466.53	444.84	427.21	414.95	421.57	433.64	447.48
5	8.6	543.87	517.17	493.3	470.55	448.96	432.05	420.41	427.7	440.52	455.06
6	8.48	547.54	520.95	497.42	474.91	453.41	437.15	426.12	433.98	447.48	462.64
7	8.36	551.66	525.15	501.91	479.6	458.19	442.52	432.06	440.41	454.53	470.24
8	8.24	556.15	529.75	506.77	484.63	463.31	448.15	438.26	446.98	461.65	477.84
9	8.12	561.05	534.77	512.00	489.99	468.76	454.05	444.69	453.71	468.85	485.46
10	8	566.33	540.20	517.59	495.68	474.55	460.22	451.37	460.58	476.13	493.09
11	7.88	572.02	546.04	523.56	501.7	480.66	466.65	458.29	467.61	483.5	500.72
12	7.76	578.11	552.29	529.89	508.06	487.11	473.35	465.46	474.79	490.94	508.37
13	7.64	584.59	558.96	536.58	514.75	493.9	480.31	472.87	482.11	498.47	516.02
14	7.52	591.47	566.04	543.65	521.78	501.01	487.54	480.53	489.54	506.08	523.68
15	7.4	598.75	573.53	551.08	529.13	508.46	495.04	488.42	497.21	513.77	531.36
16	7.28	606.42	581.44	558.88	536.82	516.24	502.81	496.57	504.98	521.54	539.04
17	7.16	614.5	589.75	567.05	544.85	524.36	510.84	504.95	512.91	529.39	546.73
18	7.04	622.97	598.48	575.58	553.21	532.81	519.14	513.58	520.98	537.32	554.44
19	6.92	631.85	607.62	584.49	561.9	541.59	527.7	522.45	529.21	545.33	562.15
20	6.8	641.11	617.18	593.76	570.92	550.7	536.53	531.57	537.58	553.42	569.87

Starting from these results, the graphical representation of the 3D variation of the Von Mises $\sigma(n_a, T)$ stress is given in the Figure 7, computed using Microsoft Excel 2017 software [44].
For the constant working temperatures, with a interval of ΔT = 10 ^{0}C from the temperature range, the variation of the Von Mises stress $\sigma(T = ct, n_a)$ is shown in Figure 8 and for n_a = constant, with the variable temperature, the variation of stress $\sigma(T, n_a = ct)$ is given in Figure 9.
The superior view of the dependence surfaces $\sigma(n_a, T)$ is shown in Figure 10.

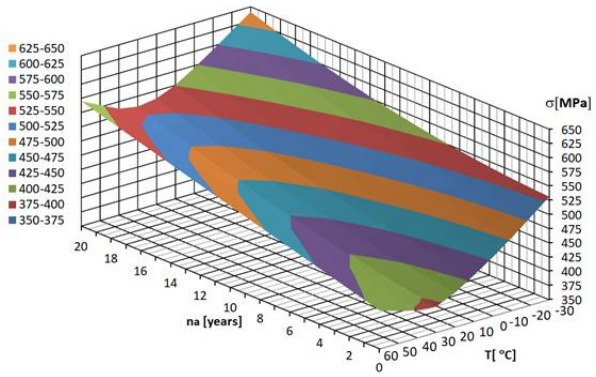

Fig. 7. The Von Mises stress $\sigma(n_a, T)$

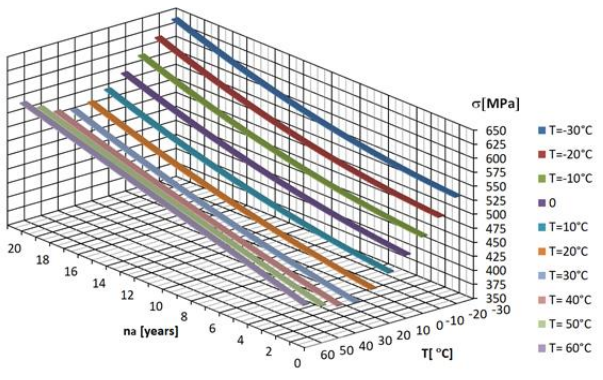

Fig. 8. The Von Mises stress $\sigma(n_a, T=ct.)$

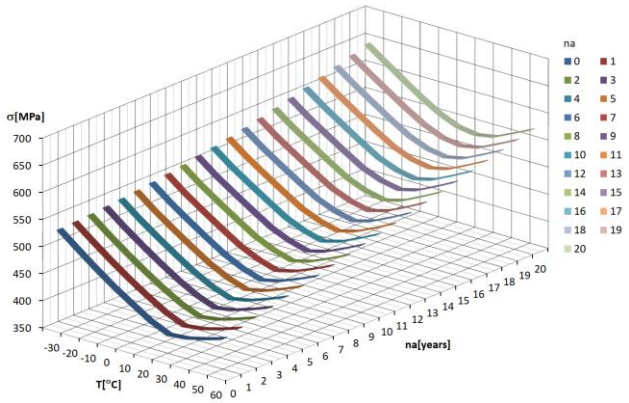

Fig. 9. The Von Mises stress $\sigma(n_a = ct., T)$

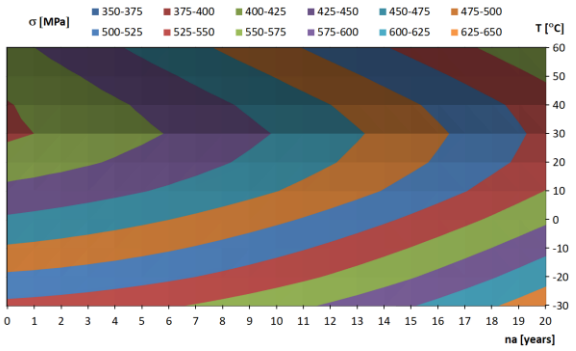

Fig. 10. The superior view of Von Mises stress $\sigma(n_a, T)$

Further study directions of the variation of the stress starting from the results given in Table 1, are the following:
a) the influence of the corrosion variation on the stress, with s = variable and T = constant, which is shown in Figure 11;
b) the influence of the temperature variation on the stress, with T = variable and s = constant, which is shown in Figure 13;
c) the combined corrosion-temperature influence on the stress, $\sigma(T, n_a)$ which are shown in Figures 7 to 10.

2.2. Study of corrosion influence on the resulting stress Von Mises

The corrosion for a given time, establishes through n_a a value of the cover thickness.
In the Figure 11 for different temperature values with T = constant, it is shown the graphs and laws of the variance of resulting Von Mises stress $\sigma(T = ct, n_a)$, calculated through an polynomial interpolation using Microsoft Excel 2017 [44] and Maple 2016 software applications [45].

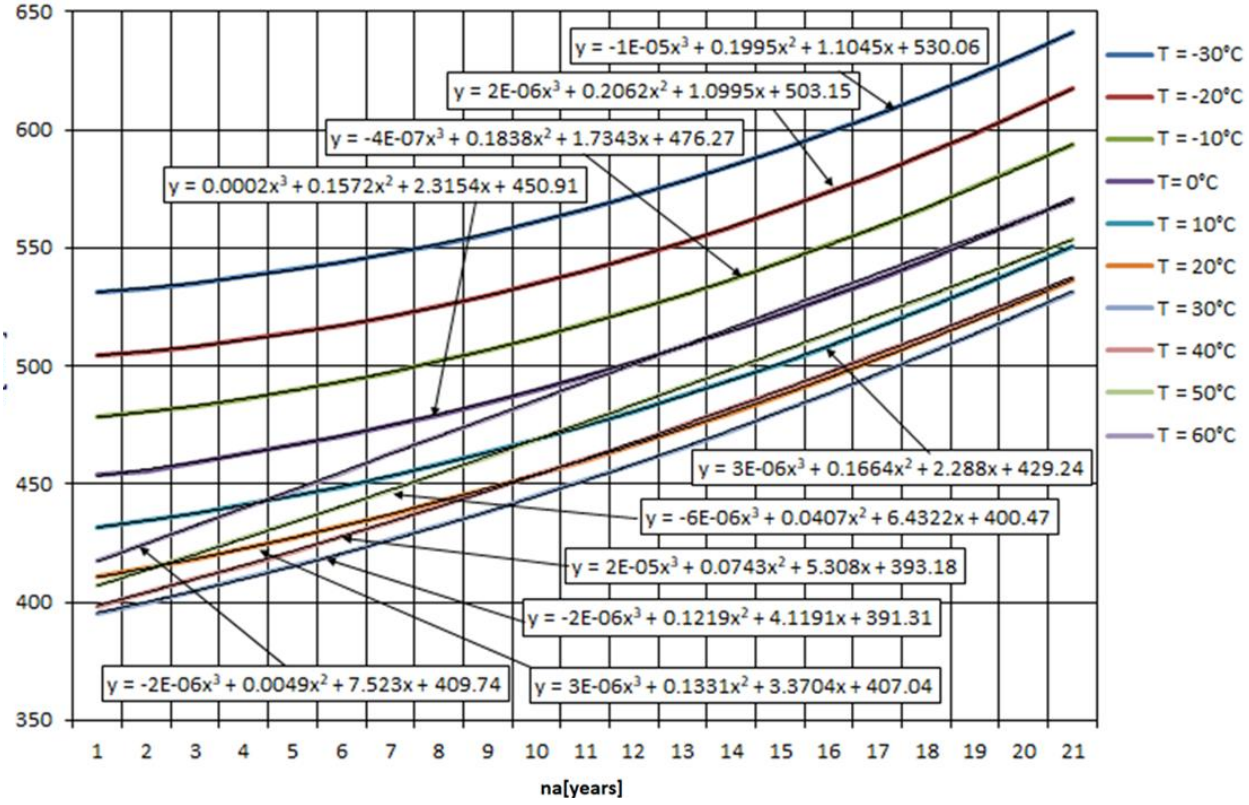

Fig. 11. The 2D graphs of Von Mises stress $\sigma(n_a, T=ct)$

In practice, this operating case occurs in controlled temperature environments, such as in the case of thermostated halls or warehouses.

The percentage decrease of Von Mises stress for (T_K = ct), with n_a =variable, $\Delta\sigma(n_a)$, taking the maximum stress from T = 60 ^{0}C as the basis of calculation, and the graph of these curves in given in Figure 12, computed using Microsoft Excel 2017 software [44].

The percentage decrease of the Von Mises stress, for (n_{aK} = ct,) with T = variable, taking as the basis for calculation the maximum stress $\Delta\sigma(T)$, that exists at T= -30 ^{0}C, is shown in Figure 13.

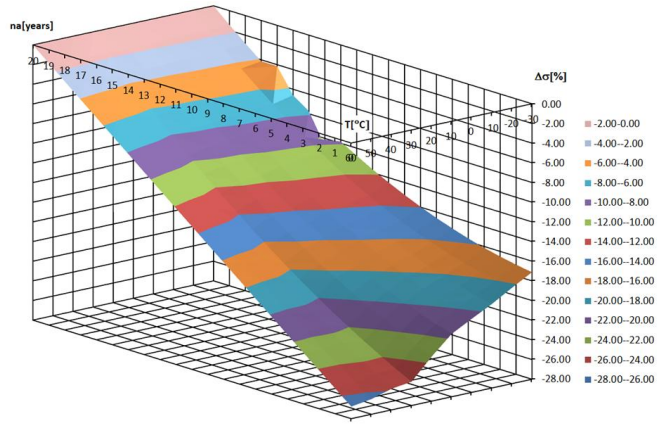

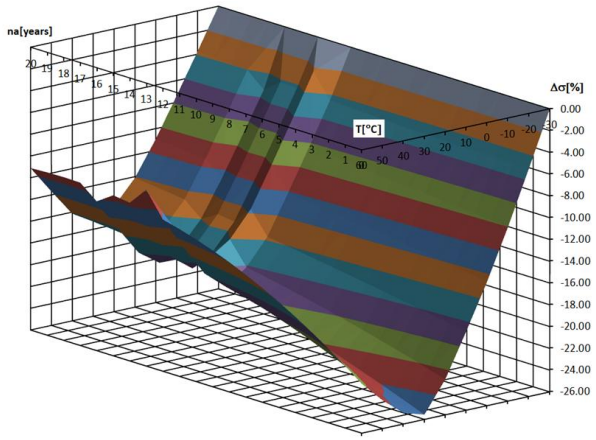

Fig. 12. The Von Mises stress variation $\Delta\sigma(n_a,T=ct.)$ **Fig. 13.**The Von Mises stress variation $\Delta\sigma(n_a=ct.,T)$

2.3. The study of the influence of temperature on the resulting stress Von Mises

Knowing the temperature variation between the operating limits T = -30 ^{0}C ... 60 ^{0}C and for constant thicknesses between in the limits: s = 7.6 ... 10 mm, according to Table 1, the laws of variation of stress were determined by polynomial interpolation, computed using Microsoft Excel 2017 software. The graphs of these curves are shown in Figure 14.

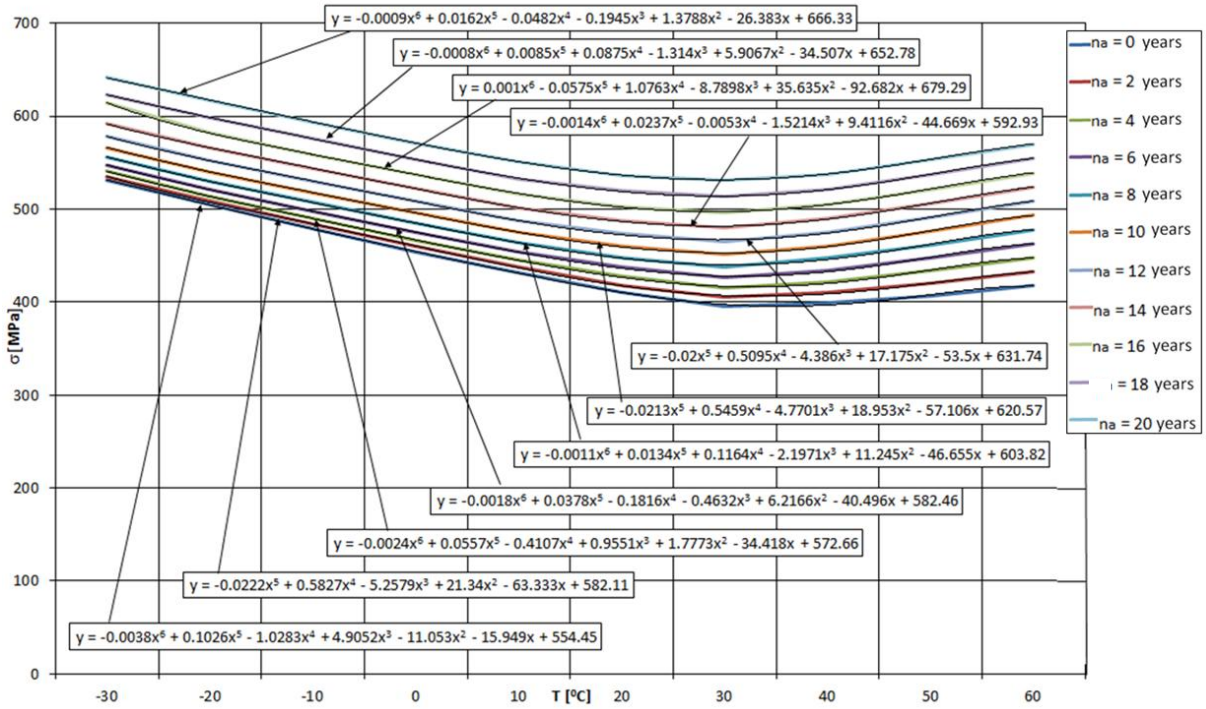

Fig. 14. The 2D graphs of Von Mises stress $\sigma(n_a = ct,T)$

As the cover has to provide the stress resistance over the entire exploitation range, the stress variation graphs from the beginning of n = 0 years and the end of the exploitation period n_a = 20 years are shown in Figure 15.

The effort difference $\Delta\sigma = \sigma_{na = 20\ years} - \sigma_{na = 0\ years}$, which appears between the beginning and the end of the exploitation period is represented graphically in Figure 16, and the law of variation is calculated by polynomial interpolation.

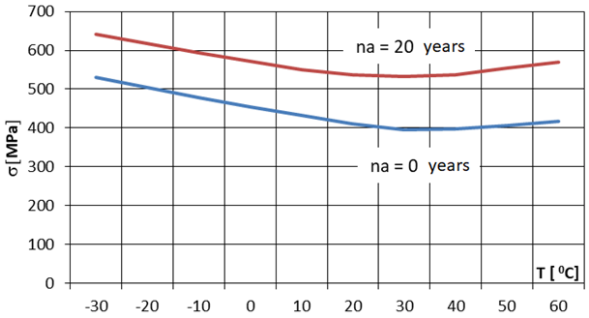

Fig. 15. The Von Mises stress at n_a = 0 years and n_a = 20 years

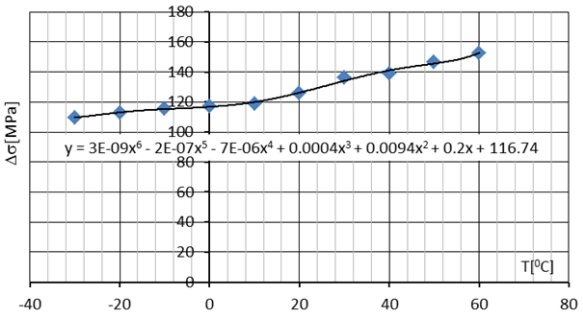

Fig. 16. The variation of Von Mises stress diference $\Delta\sigma = \sigma_{na = 20\ years} - \sigma_{na = 0\ years}$

3. Discussion

The increase of corrosion during the exploitation period, causes the thickness cover to decrease with the Δs = 26.09 %, which results in increased unitary Von Mises stress, (according to Table 1).
Following the correction of the optimized thickness and the choice of the sheet metal with an immediate superior thickness, the cover receives a thickness supplement equal to Δs = 0.75 mm, which makes the maximum effective Von Mises stress to be less than the calculated maximum stress to optimization.
The maximum unitary Von Mises stress occur at the negative temperature of T = -30 ^{0}C irrespective of the moment of exploitation n_a, (as shown in Figures 7 to 11).
At n_a = ct., the graph of the dependence of stress variation σ(T) from the Figure 14 has a minimum for the temperature T = 30 ^{0}C; the stress decreases with the temperature rise from the maximum value of T = -30 ^{0}C to the minimum value of T = 30 ^{0}C, then rises again to the temperature T = 60 ^{0}C, but below the maximum stress reached at the temperature of T = -30 ^{0}C.
For T = ct., with n_a = variable (as shown in Figure 11), shows that the evolution of corrosion determines the increase of the stress from the positive temperatures to the negative temperatures; the minimum stress being at T = 60 ^{0}C and the maximum stress it is at T = -30 ^{0}C.
The variance of the stress difference between the end and the beginning of the exploitation period, is comprised between the limits $\Delta\sigma$ = 115 up to 152 MPa, having an increasing character over the entire interval of temperature variation, (according to Figure 10).
In case of the variation stress $\Delta\sigma(n_a)$, at T = ct., it has the maximum value of $\Delta\sigma(n_a)$ = - 26.78 % for n_a = 0 years and at the temperature of T = 60 ^{0}C, (according to Figure 12).
For $\Delta\sigma$(T), at n_a = ct., (according Fig. 14), it has the maximum value of $\Delta\sigma$(T) = - 25.65 %, at n_a = 0 years and T = 30 ^{0}C.
Concerning to the state of stress that can be reached up to the admissible limits of the material cover (σ_a = 710 N/mm^2 and σ_r = 1100 N/mm^2), due to the maximum working pressure and the explosion pressure, influenced by the growth of corrosion and temperature variation, it is found that both pressures decrease.
At the beginning of the operating period, when n_a = 0 years, the pressure of the cover, which is initially higher by Δp = 151.66 % than the hydraulic pressure test, decreases with Δp = 249.33 %, until the end of the exploitation period, n_a = 20 years, and the explosion pressure which is also initially greater than Δp = 249.33 %, also decreases with Δp_{max} = 22.68 %.

4. Conclusions

This paper presents a study concerning the simultaneous influence of temperature and corrosion on Von Mises efforts in the lateral cylindrical cover of a pressurized fuel tank. In the calculation a parameterized model sectioned into ¼ of the initial model was used. The lateral cover was optimally dimensioned at mechanical stresses, with the additional minimum mass condition.

The CAD simulation on the Von Mises effort state was done and the 3D variation of the stress $\sigma(n_a, T)$ was studied together with the particular cases of variation for $\sigma(n_a = ct, T)$ and $\sigma(n_a, T = ct)$, at the same time determining the polynomials of variation through interpolation.
The final conclusion is that the influence of corrosion and temperature on the Von Mises efforts in the side cover is important and cannot be neglected in design process.

Financial disclosure: The author has no financial or proprietary interest in any material or method mentioned.
Competing interests: The author declare that he has no significant competing financial, professional or personal interests that might have influenced the performance or presentation of the study.

References

[1] A.C. Nedelcu, "Romanian automotive industry – analysis made from the intellectual capital perspective", Revista Economica, vol. 67, no. 5, pp. 80-89, 2015;
[2] A. Misztal, N. Belu, N. Rachieru, "Comparative Analysis of Awareness and Knowledge of APQP Requirements in Polish and Romanian Automotive Industry", Applied Mechanics and Materials, vol. 657, pp. 981-985, 2014;
[3] A. Hagiu, M. Platis, "The evolution of the Romanian car industry and its position on European market", STUDIA UBB NEGOTIA, vol. 57 (LVII), 2, pp. 65 - 91, 2012;
[4] G. Matache, C. Cristescu, C. Dumitrescu, V. Miroiu, "Pregătirea specialiștilor în vederea adaptabilității și creșterii competitivității", Magazine of Hydraulics, Pneumatics, Tribology, Ecology, Sensorics, Mechatronics (HIDRAULICA), no. 3-4, pp. 7-14, 2012. ISSN 1453-7303;
[5] Chen Shr-Hung, "Novel design and optimization of vehicle's natural gas fuel tank". Master's Thesis presented to the Faculty of the College of the Engineering and Technology, Ohio University, March 1997;
[6] E. Lisowski, W. Czyzycki, "Transport and storage of LNG in container tanks", Journal of KONES Powertrain and Transport, vol. 18, no. 3, pp. 193-201, 2011;
[7] M.C. Ghiţă, A.C. Micu, M. Ţălu, Ş. Ţălu, "Shape optimization of vehicle's methane gas tank", Annals of Faculty of Engineering Hunedoara - International Journal of Engineering, Hunedoara, Tome X, Fascicule 3, pp. 259-266, 2012;
[8] M.C. Ghiţă, A.C. Micu, M. Ţălu, Ş. Ţălu, E. Adam, "Computer-Aided Design of a classical cylinder gas tank for the automotive industry", Annals of Faculty of Engineering Hunedoara - International Journal of Engineering, Hunedoara, Tome XI, Fascicule 4, pp. 59-64, 2013;
[9] M.C. Ghiţă, A.C. Micu, M. Ţălu, Ş. Ţălu, "3D modelling of a gas tank with reversed end up covers for automotive industry", Annals of Faculty of Engineering Hunedoara - International Journal of Engineering, Hunedoara, Tome XI, Fascicule 3, 2013, pp. 195-200, 2013;
[10] M.C. Ghiţă, A.C. Micu, M. Ţălu, Ş. Ţălu, "3D modelling of a shrink fitted concave ended cylindrical tank for automotive industry". Acta Technica Corviniensis – Bulletin of Engineering, Hunedoara, Romania, Tome VI, Fascicule 4, pp. 87-92, 2013;
[11] M.C. Ghiţă, C.Ş. Ghiță, Ş. Ţălu, S. Rotaru, "Optimal design of cylindrical rings used for the shrinkage of vehicle tanks for compressed natural gas", Annals of Faculty of Engineering Hunedoara - International Journal of Engineering, Hunedoara, Tome XII, Fascicule 3, pp. 243-250, 2014;
[12] M.C. Ghiţă, A.C. Micu, M. Ţălu, Ş. Ţălu, "Shape optimization of a thoroidal methane gas tank for automotive industry", Annals of Faculty of Engineering Hunedoara - International Journal of Engineering, Hunedoara, Tome X, Fascicule 3, pp. 295-297, 2012;
[13] M.V.J. Bhavana, Rao S. Janardhana, B A.N. Murthy, "Design and analysis of horizontal LPG storage pressure vessel for variable dimensional constraints under given physical parameters", International Journal & Magazine of Engineering, Technology, Management and Research, vol. 4, issue 5, pp. 342 - 351, 2017;
[14] Ș. Ţălu, "Limbajul de programare AutoLISP. Teorie şi aplicaţii", (AutoLISP programming language. Theory and applications), Cluj-Napoca, Risoprint Publishing house, 2001;
[15] Ș. Ţălu, "AutoCAD 2005", Cluj-Napoca, Risoprint Publishing house, 2005;
[16] Ş. Ţălu, "Geometrie descriptivă" (Descriptive geometry), Cluj-Napoca, Risoprint Publishing house, 2010;
[17] A. Florescu-Gligore, M. Orban Ş. Ţălu, "Cotarea în proiectarea constructivă şi tehnologică" (Dimensioning in technological and constructive engineering graphics), Cluj-Napoca, Lithography of The Technical University of Cluj-Napoca, 1998;
[18] A. Florescu-Gligore, Ş. Ţălu, D. Noveanu, "Reprezentarea şi vizualizarea formelor geometrice în desenul industrial" (Representation and visualization of geometric shapes in industrial drawing), Cluj-Napoca, U. T. Pres Publishing house, 2006;
[19] Ş. Ţălu, C. Racocea, "Reprezentări axonometrice cu aplicaţii în tehnică" (Axonometric representations with applications in technique), Cluj-Napoca, MEGA Publishing house, 2007;

[20] C. Racocea, Ş. Ţălu, "Reprezentarea formelor geometrice tehnice în axonometrie" (The axonometric representation of technical geometric shapes), Cluj-Napoca, Napoca Star Publishing house, 2011;
[21] Carlos Martines Ortiz, "2D and 3D shape descriptors". Thesis for the degree of Doctor of Philosophy in Computer Science, University of Exeter, GBR, 2010;
[22] Ş. Ţălu, M. Ţălu, "A CAD study on generating of 2D supershapes in different coordinate systems", Annals of Faculty of Engineering Hunedoara - International Journal of Engineering, Hunedoara, Tome VIII, Fascicule 3, pp. 201-203, 2010;
[23] Ş. Ţălu, M. Ţălu, "CAD generating of 3D supershapes in different coordinate systems", Annals of Faculty of Engineering Hunedoara - International Journal of Engineering, Hunedoara, Tome VIII, Fascicule 3, pp. 215-219, 2010;
[24] Ş. Ţălu, "CAD representations of 3D shapes with superellipsoids and convex polyhedrons", Annals of Faculty of Engineering Hunedoara - International Journal of Engineering, Hunedoara, Tome IX, Fascicule 3, 2011, pp. 349-352, 2011;
[25] Ş. Ţălu, "Study on the construction of complex 3D shapes with superellipsoids and supertoroids", Annals of Faculty of Engineering Hunedoara - International Journal of Engineering, Hunedoara, Tome IX, Fascicule 3, pp. 299-302, 2011;
[26] Ş. Ţălu, "Complex 3D shapes with superellipsoids, supertoroids and convex polyhedrons", Journal of Engineering Studies and Research, Bacău, vol. 17, no. 4, pp. 96-100, 2011;
[27] Ş. Ţălu, "Generation of 3D shapes with superellipsoids, supertoroids, super cylinders and super cones", Journal of Engineering Studies and Research, Bacău, vol. 18, no. 2, pp. 135-139, 2012;
[28] Ş. Ţălu, M. Ţălu, "AutoCAD 2006. Proiectare tridimensională" (AutoCAD 2006. Three-dimensional designing), Cluj-Napoca, MEGA Publishing house, 2007;
[29] Ş. Ţălu, "Reprezentări grafice asistate de calculator" (Computer assisted graphical representations), Cluj-Napoca, Osama Publishing house, 2001;
[30] Ş. Ţălu, "Grafică tehnică asistată de calculator" (Computer assisted technical graphics), Cluj-Napoca, Victor Melenti Publishing house, 2001;
[31] Ş. Ţălu, "AutoCAD 2017", Cluj-Napoca, Napoca Star Publishing house, 2017;
[32] T. Niţulescu, Ş. Ţălu, "Aplicaţii ale geometriei descriptive şi graficii asistate de calculator în desenul industrial" (Applications of descriptive geometry and computer aided design in engineering graphics), Cluj-Napoca, Risoprint Publishing house, 2001;
[33] C. Bîrleanu, Ş. Ţălu, "Organe de maşini. Proiectare şi reprezentare grafică asistată de calculator" (Machine elements. Designing and computer assisted graphical representations), Cluj-Napoca, Victor Melenti Publishing house, 2001;
[34] Ş. Ţălu, "Micro and nanoscale characterization of three dimensional surfaces. Basics and applications", Napoca Star Publishing House, Cluj-Napoca, Romania, 2015;
[35] M. Țălu, "Calculul pierderilor de presiune distribuite în conducte hidraulice" (Calculation of distributed pressure loss in hydraulic pipelines), Craiova, Universitaria Publishing house, 2016;
[36] M. Țălu, "Pierderi de presiune hidraulică în conducte tehnice cu secțiune inelară. Calcul numeric și analiză C.F.D." (Hydraulic pressure loss in technical piping with annular section. Numerical calculation and C.F.D.), Craiova, Universitaria Publishing house, 2016;
[37] M. Ţălu, "Mecanica fluidelor. Curgeri laminare monodimensionale" (Fluid mechanics. The monodimensional laminar flow), Craiova, Universitaria Publishing house, 2016;
[38] M. Rusănescu, "Material requirements planning, inventory control system in industry", Magazine of Hydraulics, Pneumatics, Tribology, Ecology, Sensorics, Mechatronics (HIDRAULICA), no. 1, pp. 21-25, 2014. ISSN 1453-7303;
[39] Ș. Ţălu, M. Ţălu, "The influence of deviation from circularity on the stress of a pressurized fuel cylindrical tank", Magazine of Hydraulics, Pneumatics, Tribology, Ecology, Sensorics, Mechatronics (HIDRAULICA), no. 4, pp. 34-45, 2017, ISSN 1453-7303;
[40] D. Vintilă, M. Ţălu, Ș. Ţălu, "The CAD analyses of a torospheric head cover of a pressurized cylindrical fuel tank after the crash test", Magazine of Hydraulics, Pneumatics, Tribology, Ecology, Sensorics, Mechatronics (HIDRAULICA), no. 4, pp. 57-66, 2017, ISSN 1453-7303;
[41] M. Bică, M. Ţălu, Ș. Ţălu, "Optimal shapes of the cylindrical pressurized fuel tanks", Magazine of Hydraulics, Pneumatics, Tribology, Ecology, Sensorics, Mechatronics (HIDRAULICA), no. 4, pp. 6-17, 2017, ISSN 1453-7303;
[42] *** Autodesk AutoCAD 2017 software;
[43] *** SolidWorks 2017 software;
[44] *** Microsoft Excel 2017 software;
[45] *** Maple 2016 software.

.